



PARAMETER IDENTIFICATION OF PHOTOVOLTAIC MODELS USING ENHANCED CRAYFISH OPTIMIZATION ALGORITHM WITH OPPOSITION-BASED LEARNING STRATEGIES

Burçin ÖZKAYA^{1*}


¹Bandırma Onyedi Eylül University, Faculty of Engineering and Natural Sciences, Department of Electrical Engineering, 10200, Bandırma, Türkiye

Abstract: Recently, solar energy has become an attractive topic for researchers as it has been preferred among renewable energy sources due to its advantages such as unlimited energy supply and low maintenance expenses. The precise modeling of the solar cells and the model's parameter estimate are two of the most important and difficult topics in photovoltaic systems. A solar cell's behavior can be predicted based on its current-voltage characteristics and unknown model parameters. Therefore, many meta-heuristic search algorithms have been proposed in the literature to solve the PV parameter estimation problem. In this study, the enhanced crayfish optimization algorithm (ECO) with opposition-based learning (OBL) strategies was proposed to estimate the parameters of the three different PV modules. A thorough simulation study was conducted to demonstrate the performance of the ECO algorithm in tackling benchmark challenges and PV parameter estimate problems. In the first simulation study, using three OBL strategies, six variations of the COA were created. The performances of these variations and the classic COA have been tested on CEC2020 benchmark problems. To determine the best COA variation, the results were analyzed using Friedman and Wilcoxon tests. In the second simulation study, the best variation, called ECO, and the base COA were applied to estimate the parameters of three PV modules. According to the simulation results, the ECO algorithm achieved 1.0880%, 37.8378%, and 0.8106% lower error values against the base COA for the parameter estimation of the STP6-120/36, Photowatt-PWP201, and STM6-40/36 PV modules. Moreover, the sensitivity analysis was performed in order to determine the parameters influencing the PV module's performance. Accordingly, the change in the photo-generated current and diode ideality factor in the single-diode model affects the performance of PV modules the most. The comprehensive analysis and results showed the ECO's superior performance in parameter estimation of three PV modules compared to other algorithms found in the literature.

Keywords: PV parameter estimation, Single-diode model, Enhanced crayfish optimization algorithm, Opposition-based learning strategy

*Corresponding author: Bandırma Onyedi Eylül University, Faculty of Engineering and Natural Sciences, Department of Electrical Engineering, 10200, Bandırma, Türkiye

E mail: bozkaya@bandirma.edu.tr (B. ÖZKAYA)

Burçin ÖZKAYA  <https://orcid.org/0000-0002-9858-3982>

Received: May 27, 2024

Accepted: July 12, 2024

Published: July 15, 2024

Cite as: Özkaya B. 2024. Parameter identification of photovoltaic models using enhanced crayfish optimization algorithm with opposition-based learning strategies. BSJ Eng Sci, 7(4): 771-784.

1. Introduction

Recently, the development and application of renewable energy have become more important due to the rising consumption of non-renewable energy sources and their associated environmental pollution. The abundance and low pollution of solar energy, especially, make it stand out (Wang et al., 2022). The utilization of solar energy is crucial for improving the ecological environment since it may be used to generate electricity or thermal energy without the need for fuel or water, nor does it produce pollution (Yang et al., 2020). Many researchers have undertaken various studies in order to address and overcome the problems in PV systems, where the aim is to decrease the total costs while increasing efficiency. PV systems must be thoroughly investigated and analyzed from a variety of perspectives as their popularity develops (Naeijian et al., 2021). The precise and effective modeling of solar cells is one of the most important and

difficult aspects of PV systems. The main cause of this problem is the nonlinear properties of the solar cells and the lack of complete parameter availability. Therefore, a precise model needs to be developed to accurately study and assess the real behavior of PV systems (Yang et al., 2020).

In the literature, a number of mathematical models, the most prominent of which is the diode-based model, have been developed to characterize PV properties under various operating conditions. The most well-known PV models presented in the literature are the PV module model, single diode, double diode, and triple diode models (Naeijian et al., 2021). The modeling of the solar PV system includes parameter identification and mathematical formulations. Unfortunately, the lack of easy access to these parameter values restricts the usefulness of these models. This problem, which is inaccurate parameter identification, can lead to



significant errors in performance evaluation, quality control, and maximum power point tracking of PV systems. Therefore, the accurate model parameters, such as the number of diodes, ideality factor, series resistances, and shunt resistances, are necessary for correct results. Thus, the accurate parameter extraction of the solar cells is a growingly significant issue for researchers (Wang et al., 2022).

Many methods have been presented in the literature to determine the parameters of PV cells, which are classified as analytical, iterative, and meta-heuristic algorithms (Wang et al., 2022). Analytical methods use complicated mathematical equations to calculate these values and can be easily implemented (Cárdenas et al., 2016). However, they have significant drawbacks, such as the requirement for particular mathematical features and assumptions. These assumptions can occasionally cause significant errors or affect the accuracy of the solutions (Chenche et al., 2018). Iterative algorithms, such as Newton-Raphson and Lambert W-functions, rely heavily on initial guesses and gradient information. These methods require the equations of the system to be continuous, convex, and differentiable, which limits their usefulness (Ortiz-Conde et al., 2006; Ayang et al., 2019). To solve the drawbacks of the first two methods, meta-heuristic search (MHS) algorithms have gained popularity for determining PV cell parameters due to their improved performance in nonlinear and complex optimizations.

In the literature, many studies have been carried out to identify the parameters of the PV cell. A hybrid algorithm incorporating the trust-region reflective algorithm and the artificial bee colony algorithm was introduced to estimate the PV model (Wu et al., 2018). The authors used the slime mould optimization algorithm to estimate the PV cell parameters, where three diode model were considered (Kumar et al., 2020). An improved version of the whale optimization algorithm using the refraction-learning strategy was presented for parameter estimation of the PV model, where only the single-diode PV model was considered (Long et al., 2020). The authors used the transient search algorithm to solve the PV parameter estimation problem. Here, only the parameters of the triple-diode model were determined under changing temperatures and solar irradiance (Qais et al., 2020). An improved version of the Harris Hawks optimization algorithm was introduced to extract the model parameters of PV, where four diode model and two different commercial PV cells (Naeijian et al., 2021). An improved equilibrium optimizer was proposed to determine the unknown parameters of the PV models. In this study, the simulations were carried out under constant conditions, and under partial shading and changing weather conditions (Wang et al., 2021). An improved JAYA algorithm based on chaotic learning methods was proposed for parameter identification of PV cells (Premkumar et al., 2021). The authors proposed a heterogeneous differential evolution algorithm to

identify the parameters of PV cells, where six different PV modules were considered (Wang et al., 2022). An improved moth flame optimization algorithm based on opposition-based learning method was proposed to estimate the parameters of the PV cell. The parameters of the three commercial PV cell were extracted using the reported algorithm (Sharma et al., 2022). To extract the PV cell/module parameters, an improved version of the teaching-learning-based artificial bee colony algorithm using fitness-distance balance method was proposed (Duman et al., 2022). A hybrid seagull optimization algorithm was presented to identify the parameters of PV models for the SD, DD, and PV module models (Long et al., 2022). An enhanced gradient-based optimization algorithm by using the orthogonal learning mechanism was proposed to estimate the PV model parameters. Here, the experiments were carried out using the four PV models and two commercial PV modules (Yu et al., 2022). To specify the parameters of the two types of PV cell, the atomic orbital search algorithm was used (Ali et al., 2023). The authors presented a comprehensive analysis on the PV parameter estimation using eight MHS algorithms for three types of PV models (Navarro et al., 2023). In another study, an improved version of Harris Hawks optimization algorithm was introduced for determining the unknown parameters of the three diode model. In the study, the parameters of the most commonly used commercial PV cell and PV module were estimated using the proposed algorithm (Garip, 2023). To estimate the parameters of the three types of PV models, the chimp optimization algorithm was used (Yang et al., 2023). The authors used the northern goshawk optimization algorithm for identifying the PV model parameters, where only the three diode model was considered (El-Dabah et al., 2023). An improved moth flame algorithm including the local escape operators was proposed to estimate the PV model parameters (Qaraad et al., 2023). The ranking teaching-learning-based optimization to solve the PV parameter estimation problem. In the study, three types of commercial PV modules were used to show the efficiency of the proposed algorithm (Yu et al., 2023). The authors used a squirrel search algorithm for the estimation of PV parameters. Here, the simulation study was performed under two case study, where R.T.C. France silicon solar cell and polycrystalline CS6P-220P solar module (Maden et al., 2023). The artificial hummingbird algorithm was used to estimate the electrical parameters of the single- and double-diode PV cell (El-Sehiemy et al., 2023). A hybrid optimization algorithm including white shark optimizer and artificial rabbit optimization was proposed to extract two PV cells and six PV modules (Çetinbaş et al., 2023). The authors proposed an enhanced version of the artificial gorilla troops optimizer to estimate the parameters of two PV module (Shaheen et al. 2023). The artificial humming bird algorithm for solving the parameter estimation of the PV models was presented, where two different PV module were carried out

(Ayyarao and Kishore, 2024). A multi-strategy gaining-sharing knowledge-based algorithm was introduced to identify the unknown parameters of the PV modules (Xiong et al. 2024). The author used the weighted leader search algorithm for estimating the parameters of the PV cells and modules (Çetinbaş, 2024). An enhanced prairie dog optimization algorithm was proposed to determine the parameters of the PV model (Izci et al., 2024).

In this study, an enhanced crayfish optimization algorithm (ECOA) based on opposition-based learning (OBL) strategies was proposed to solve the PV parameter estimation problem and benchmark problems. Three OBL strategies were applied to improve the exploration ability of the COA. Using these OBL strategies, six variations of the COA using these OBL strategies were created. To validate the ECOA's performance, a complete simulation study was conducted using the benchmark problems and PV parameter estimation problems. In the first simulation study, all variations and the base COA were implemented for solving the CEC2020 (Yue et al., 2019) benchmark problems for five different dimensional search spaces (10/20/30/50/100). The performance of them was compared using the statistical analysis methods, and the best COA variation was selected. In the second experimental study, the ECOA and the base COA were applied to solve the PV parameter estimation problem. Here, only single-diode PV cell model was used. Three case studies using the PV module, including Photowatt-PWP201, STP6-120/36, and STM6-40/36, were considered. Their results were compared with the reported results in the literature.

The contributions of this paper to the literature are as follows:

- An improved crayfish optimization algorithm based on opposition-based learning strategies was proposed to the literature as a strong MHS algorithm.
- A comprehensive experimental study was performed to validate the performance of the proposed ECOA for solving both benchmark problems and PV parameter estimation problems.
- The proposed ECOA presented the best optimal solutions in the literature for solving the PV parameter estimation problem.
- The sensitivity analysis was carried out to determine the effect of the unknown parameters on the objective function.

This study includes four sections after the introduction, and these are summarized accordingly. Section 2 includes two sub-sections. In the first sub-section, the mathematical model of the PV cell or module and the formulation of the PV parameter extraction problem are presented. In the second sub-section, the proposed ECOA is explained. Section 3 analyzes and presents the simulation results of the benchmark problems and PV models of the three PV modules. Section 4 presents the conclusions.

2. Materials and Methods

This section consists of two sub-sections. In the first sub-section, the mathematical model of the PV module and the formulation of the objective function considered in the PV parameter estimation problem are described. In the second sub-section, the proposed ECOA is presented.

2.1. Mathematical Model of the PV cell and Problem Formulation

The behavior of photovoltaic (PV) cells and modules has been modeled by many mathematical formulas and the most popular of which is the diode model. This is due to the fact that PV cells, which are made up of semiconductor components, have an I-V curve that is exponential and resembles a diode. There are multiple parameters in every diode-based model that need to be calculated with accuracy, and the precise estimation of these parameters is essential (Wang et al., 2022).

The single-diode (SD) model is a generally used mathematical expression of a photovoltaic (PV) cell that simplifies its complex physical behavior into an equivalent electrical circuit as in Figure 1 (Wang et al., 2022). This model consists of a current source (I_{pv}) for the photocurrent produced by sunlight, a diode for the p-n junction, a series resistance (R_s) for resistive losses within the cell, and a shunt resistance (R_{sh}) for leakage currents. Accordingly, the output current (I_L) is mathematically expressed as in Equation (1) (Isen and Duman, 2024).

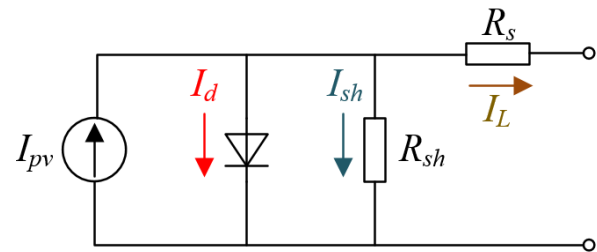


Figure 1. The equivalent circuit model of the single-diode.

$$I_L = I_{pv} - I_{sh} - I_d = I_{pv} - \frac{R_s I_L + V_L}{R_{sh}} - I_{o1} \left[\exp\left(\frac{(R_s I_L + V_L)q}{T \cdot k \cdot a}\right) - 1 \right] \quad (1)$$

Here, V_L , I_{sh} , I_d , and I_{o1} represent the terminal voltage, the current passing through R_{sh} , the current passing through the diode, and the reverse saturation current of the diode, respectively. a , q , T , and k denote the ideality factor of the diode, the electron charge ($1.60217646 \times 10^{-19}$ C), the temperature in Kelvin, and the Boltzmann constant ($1.3806503 \times 10^{-23}$ J/K), respectively.

The models that are most frequently used in PV have been described above. These equations are converted into corresponding optimization problems so that an optimization algorithm can determine the parameter values with accuracy. By employing the ideal parameter values, the objective function seeks to minimize the difference between the measured and experimental data. The error function for the SD model is expressed as in Equation (2), where x is the decision variables (Wang et

al., 2022).

$$\begin{cases} f(V_L, I_L, x) = I_{pv} - \frac{R_s I_L + V_L}{R_{sh}} - I_{o1} \left[\exp\left(\frac{(R_s I_L + V_L)q}{T \cdot k \cdot a}\right) - 1 \right] - I_L, \\ x = \{a, R_s, R_{sh}, I_{pv}, I_{o1}\} \end{cases} \quad (2)$$

The objective function used in this study is the total root mean square error (RMSE), which serves to quantify the difference between the observed and simulated results. The mathematical expression of the objective function considered in this study is evaluated by Equation (3), where m is the experimental I - V data and f_{obj} represents the objective function (Wang et al., 2022).

$$\text{Minimize } f_{obj}(x) = \sqrt{\frac{1}{m} \sum_{j=1}^m f(V_L, I_L, x)^2} \quad (3)$$

2.2. Method

2.2.1. Overview of the Crayfish Optimization Algorithm

The Crayfish Optimization Algorithm (COA) proposed in the literature draws inspiration from the foraging, summer vacationing, and competitive behaviors of the crayfish. It includes two stages focused on exploitation (foraging and competition) and one stage dedicated to exploration (a summer resort). The equilibrium between these stages is managed by a temperature variable (Jia et al., 2023).

The initial population for the COA involves randomly creating a set of candidate solutions (x) in the search space, where $x_{i,j}$ is the position of the i th individual in the j th dimension and is created using Equation (4). Also, LB and UB denote the lower and upper bounds of the search space, respectively (Jia et al., 2023).

$$x_{i,j} = rand \cdot (UB_j - LB_j) + LB_j \quad (4)$$

Temperature changes influence crayfish behavior, prompting them to enter various stages. When the temperature ($temp$) value is greater than 30° , the COA moves into either the competition or the summer resort stage. In the summer resort stage, the crayfish aim to get closer to the cave, representing the optimal solution. This movement towards the cave strengthens the exploitation ability of the COA. During this stage, new solutions are updated based on the positions of individual crayfish (x_i) and the cave (x_{shade}), where x_{shade} is the average of the x_G and x_L . Here, x_G and x_L represent the best solution obtained so far and the best position of the current population, respectively. The competition among crayfish for caves occurs randomly. If $rand < 0.5$, it indicates no other crayfish are vying for the caves, allowing a crayfish to directly enter the cave for its summer vacation. At this point, the crayfish will move into the cave for the summer resort stage according to Equation (5), where c_2 is a decreasing curve (Jia et al., 2023).

$$x_{i,j}^t = rand \cdot c_2 \cdot (x_{shade} - x_{i,j}^{t-1}) + x_{i,j}^{t-1} \quad (5)$$

indicates that other crayfish are also interested in the cave, leading to competition for it. The crayfish competes for the cave using Equation (6) (Jia et al., 2023).

$$x_{i,j}^t = x_{shade} + x_{i,j}^{t-1} - x_{z,j}^{t-1} \quad (6)$$

When the $temp$ is equal to or less than 30° , the crayfish will move towards the food source. Upon finding the food, they assess its size. The crayfish adjust their feeding behavior based on the size of the food, which is determined by the current solution ($fitness_{food}$) and the fitness value of it ($fitness_i$). They generate new solutions when food is suitable, considering their position, a food intake constant (p), and the food's position (x_{food}). If the food is too large, the crayfish will use their claws to tear it apart and eat it using their second and third walking legs alternately. The crayfish control the food intake, influenced by temperature and following a positive distribution. The mathematical expression of the alternating feeding of the crayfish is defined as follows in Equation 7 (Jia et al., 2023):

$$x_{i,j}^t = p \cdot (\cos(2 \cdot \pi \cdot rand) - \sin(2 \cdot \pi \cdot rand)) \cdot x_{food} + x_{i,j}^{t-1} \quad (7)$$

When the food size is deemed suitable for direct consumption by the crayfish, they move directly to the food location and start eating. The formula for this direct feeding behavior is as follows in Equation 8 (Jia et al., 2023):

$$x_{i,j}^t = x_{i,j}^{t-1} \cdot rand \cdot p + p \cdot (x_{i,j}^{t-1} - x_{food}) \quad (8)$$

During the foraging stage, crayfish employ varying feeding techniques depending on the size of their food, with food location x_{food} symbolizing the optimal solution. Progressing through this stage, the COA moves closer to the optimal solution, improving its exploitation capacity and demonstrating strong convergence capabilities.

2.2.2. Overview of the Opposition-Based Learning Strategies

Opposition-based learning (OBL) strategies in MHS algorithms aim to improve the search process by considering both the present candidate solutions and their opposites. This dual consideration increases the exploration ability, helps avoid local optima, and accelerates the convergence of optimal solutions. The algorithm can be made more effective and efficient by analyzing opposing solutions, which will produce higher-quality solutions and preserve population diversity. Ultimately, OBL enhances the overall performance of meta-heuristic algorithms by facilitating a more thorough and balanced search for optimal results (Mahdavi et al., 2018).

In the literature, different OBL strategies have been presented for improving the performance of the MHS algorithms. In this paper, three OBL strategies have been considered and are explained below:

(i) *Strategy-1*: It is the classical OBL strategy proposed in the literature and can be mathematically described in Equation (9) (Tizhoosh, 2005). Here x_j is a point in D -

dimensional search space and $\overline{x_j^o}$ is the opposite of x_j .

$$\overline{x_j^o} = ub_j - x_j + lb_j, x_j \in [lb_j, ub_j], j = 1, 2, \dots, D \quad (9)$$

(ii) *Strategy-2*: It is the quasi-opposition based learning (QOBL) strategy introduced (Rahnamayan et al., 2007). It is described as in Equation (10), where $\overline{x_j^q}$ is the quasi-opposite point of x_j and M_j is the mean value of the ub_j and lb_j . r is a random number between 0 and 1.

$$\overline{x_j^q} = \begin{cases} M_j + r \cdot (\overline{x_j^o} - M_j), & \text{if } x_j < M_j \\ \overline{x_j^o} + r \cdot (M_j - \overline{x_j^o}), & \text{otherwise} \end{cases}, j = 1, 2, \dots, D \quad (10)$$

(iii) *Strategy-3*: It is the quasi-reflection opposition based learning (QROBL) strategy proposed in the literature. It can be modeled as in Equation (11), where $\overline{x_j^{qr}}$ is the quasi-reflected point of x_j and r is a random

number between 0 and 1 (Ergezer et al., 2009).

$$\overline{x_j^{qr}} = \begin{cases} x_j + r \cdot (x_j - M_j), & \text{if } x_j < M_j \\ M_j + r \cdot (M_j - \overline{x_j^o}), & \text{otherwise} \end{cases}, j = 1, 2, \dots, D \quad (11)$$

2.2.3. Proposed Enhanced Crayfish Optimization Algorithm

Similar to the other MHS algorithms, COA might experience sluggish convergence and become stuck in a local optimum. For this reason, three OBL strategies explained in section 2.2.2 were used in the COA. These strategies were implemented in two stages in the COA. Firstly, they were applied in population initialization to increase the variety and quality of the initial population. Secondly, it was applied in the population update phase to improve the convergence performance of the algorithm.

Inputs: $N, maxFEs, D$	
Output: Best solution	
1.	Generate the initial population randomly using Equation (4).
	// Apply the OBL strategies for Case-1, Case-2, and Case-3 //
2.	Select OBL strategy.
3.	Create the oppositional population using Equation (9) for Case-1, Equation (10) for Case-2, and Equation (11) for Case-3.
4.	Compute the fitness value of the population and obtain x_G and x_L .
5.	while $FEs < maxFEs$
6.	Calculate the <i>temp</i> value.
7.	if $temp > 30^\circ$
8.	Determine the x_{shade}
9.	if $rand < 0.5$
10.	The crayfish performs the summer resort stage using Equation (5).
11.	else
12.	The crayfish competes for the cave using Equation (6).
13.	end if
14.	else
15.	The food size (Q) and food intake are determined.
16.	if $Q > 2$
17.	The crayfish rends the food and foraging according to Equation (7).
18.	else
19.	The crayfish foraging according to Equation (8).
20.	end if
21.	end if
	// Apply the OBL strategies for Case-4, Case-5, and Case-6 //
22.	Select OBL strategy.
23.	Create the oppositional population using Equation (9) for Case-4, Equation (10) for Case-5, and Equation (11) for Case-6.
24.	Compute the fitness value of the population and obtain x_G and x_L .
25.	end while

Figure 2. Algorithm-1: The pseudocode of the ECOA algorithm.

The pseudocode of the ECOA is presented in Algorithm-1 in Figure 2. According to Algorithm-1, the population initializes in line 1. Then, the OBL strategy is selected in line 2. In line 3, the oppositional population is created based on the selected OBL strategy. Accordingly, for Case-1, the oppositional population is created using the Strategy-1, where Equation (9) is used. On the other hand, for Case-2, the oppositional population of the initial population is created using the Strategy-2, where Equation (10) is used. For Case-3, the Strategy-3 is considered and Equation (11) is used to obtain the oppositional population. The oppositional population is created according to the Case-1, Case-2, or Case-3 based on the selected strategy in line 3. The fitness values of the population are computed, and x_G and x_L are determined in line 4. In lines 5 to 25, the search process life cycle of the algorithm is carried out. The $temp$ value is calculated in line 6. If $temp$ value is higher than 30° , the summer resort stage or competition stage is applied according to the $rand$ value; otherwise, the foraging stage is performed in lines 14 to 21. In line 22, the OBL strategy is selected, and the oppositional population is generated according to Case-4, Case-5 or Case-6 based on the selected strategy in line 22. For Case-4, Case-5, and Case-6, Strategy-1, Strategy-2, and Strategy-3 are considered, respectively. Lastly, the fitness values of the population are calculated, and x_G and x_L are obtained in line 24. This process continues until the stopping criterion is met.

3. Results and Discussion

In this study, to prove the performance of the ECOA, a comprehensive experimental study was performed. This section consists of two sub-sections. In the first sub-section, the six variations of and base COA were implemented to solve the CEC2020 benchmark problems in 10/20/30/50/100 dimensional search space. Using the Friedman test and convergence analysis, the best COA variation was determined. In the second sub-section, the best COA variation, called ECOA, was implemented on the PV parameter estimation problem.

3.1. Determining the Best COA Variation on Solving Benchmark Problems

In this section, the performance of the base COA and six variations of it were applied to solve the CEC2020 benchmark suite. The CEC2020 benchmark suite includes 10 benchmark problems (Yue et al., 2019). In order to ensure a fair comparison between the algorithms, the maximum number of fitness function evaluations ($maxFEs$) was set as the stopping criteria for the algorithms, which was taken as $10000 \cdot D$. Moreover, each algorithm was run 51 times for each problem. The parameter settings of the algorithm are taken as given in its original paper, and the parameters for COA variations are the same as the base COA algorithm.

In order to evaluate the results of all algorithms, the Friedman test and Wilcoxon pairwise test were carried out. The Friedman test results are presented in Table 1. In Table 1, the algorithm with the best Friedman score

for each experiment is in bold. Besides, in the last column of Table 1, the mean Friedman score value obtained from the experiments carried out in five different dimensions for each algorithm is presented. Moreover, the mean Friedman score values obtained by each algorithm in five different experiments are given in the last column of Table 1. Accordingly, Case-3 achieved the best Friedman score value among all algorithms in all experiments. Other variations were not able to exhibit as stable search performance as Case-3 against the base COA. Case-6 ranked second according to the mean score value, achieved better score values than the base COA in the 10, 30, 50, and 100 dimensions, but fell behind the COA in the 20 dimensions. On the other hand, Case-4 ranked third according to the mean score value obtained better score values than the base COA in 3 of 5 experiments.

In addition to the Friedman test, the Wilcoxon test was performed to assess the performance of the variations pairwise with the base algorithm. The results of the Wilcoxon pairwise results of the COA and its variations are presented in Table 2. To explain how to interpret the data in the table, for example, the expression "Case-1 vs. COA" indicates that a pairwise comparison is made between Case-1 and the COA. The "+" sign indicates that Case-1 is superior to the COA, the "-" sign indicates that the COA is superior to Case-1, and the "=" sign indicates that the two algorithms are equal. When the results given in Table 2 were examined, it was clearly seen that Case-3 was superior to COA in all experiments.

The convergence analysis as well as the statistical analysis methods are performed to evaluate the performance of the algorithms. The CEC2020 benchmark suite includes four problem types: unimodal, multimodal, hybrid, and composition. To evaluate the performance of the algorithms in these four different problem types, F1 (unimodal), F3 (multimodal), F6 (hybrid), and F10 (composition) were selected. The convergence curves of the six COA variations and the base COA in 20-dimensional search space are presented in Figure 3. According to the convergence graph given in Figure 3 (a), it was seen that Case-3 achieved an error value below 500 for the F1 problem compared to other algorithms. For problems F3 and F6, Case-3 achieved significantly smaller error values than its competitors. Lastly, for the F10 problem, Case-3 achieved better results than its competitors by a slight margin. To sum up, when the convergence curves for all problem types given in Figure 3 were examined, it was seen that Case-3 obtained the lowest error values among all algorithms.

The convergence graphs alone are not sufficient to evaluate the search performance of an algorithm because they are drawn based on the run in which each algorithm achieved the lowest objective function value among 51 runs. Therefore, the box-plot graphs were drawn based on the results of 51 runs of the algorithms given in Figure 4. For this, four different problem types, F1 (unimodal), F2 (multimodal), F5 (hybrid), and F9 (composition) were selected. According to box-plots of all problems given in

Figure 4, Case-3 obtained the lowest min, max, and median values among all algorithms. These results showed that Case-3 had a more stable search performance than its competitors. To sum up, when overall analysis results based on the

Friedman test, Wilcoxon test, and convergence analysis were evaluated, Case-3 outperformed its competitors in the simulation study where CEC2020 benchmark problems were solved in five different dimensions. In the remainder of the study, Case-3 was referred to as ECOA.

Table 1. Friedman score of the COA and its variations

Method	$D = 10$	$D = 20$	$D = 30$	$D = 50$	$D = 100$	Mean Score
Case-3	3.4588	3.7176	3.5784	3.4098	3.4314	3.5192
Case-6	4.0569	4.1725	3.9039	3.9706	3.8922	3.9992
Case-4	3.9510	4.1039	4.1157	4.1588	3.8941	4.0447
COA	4.0667	3.9706	4.0843	4.2039	4.0627	4.0776
Case-2	4.2745	3.9471	3.8961	4.1745	4.2333	4.1051
Case-1	4.0608	3.9608	4.2294	4.1451	4.2039	4.1200
Case-5	4.1314	4.1275	4.1922	3.9373	4.2824	4.1341

Table 2. Wilcoxon pairwise results of the COA and its variations

vs. COA (+ / = / -)	$D = 10$	$D = 20$	$D = 30$	$D = 50$	$D = 100$
Case-1	5/4/1	5/5/0	4/2/4	5/4/1	5/3/2
Case-2	3/3/4	6/4/0	6/2/2	4/4/2	4/3/3
Case-3	8/2/0	7/3/0	7/2/1	7/2/1	6/3/1
Case-4	7/3/0	4/5/1	5/3/2	5/3/2	5/3/2
Case-5	3/4/3	4/5/1	4/3/3	6/2/2	4/2/4
Case-6	6/4/0	3/4/3	5/4/1	6/2/2	6/2/2

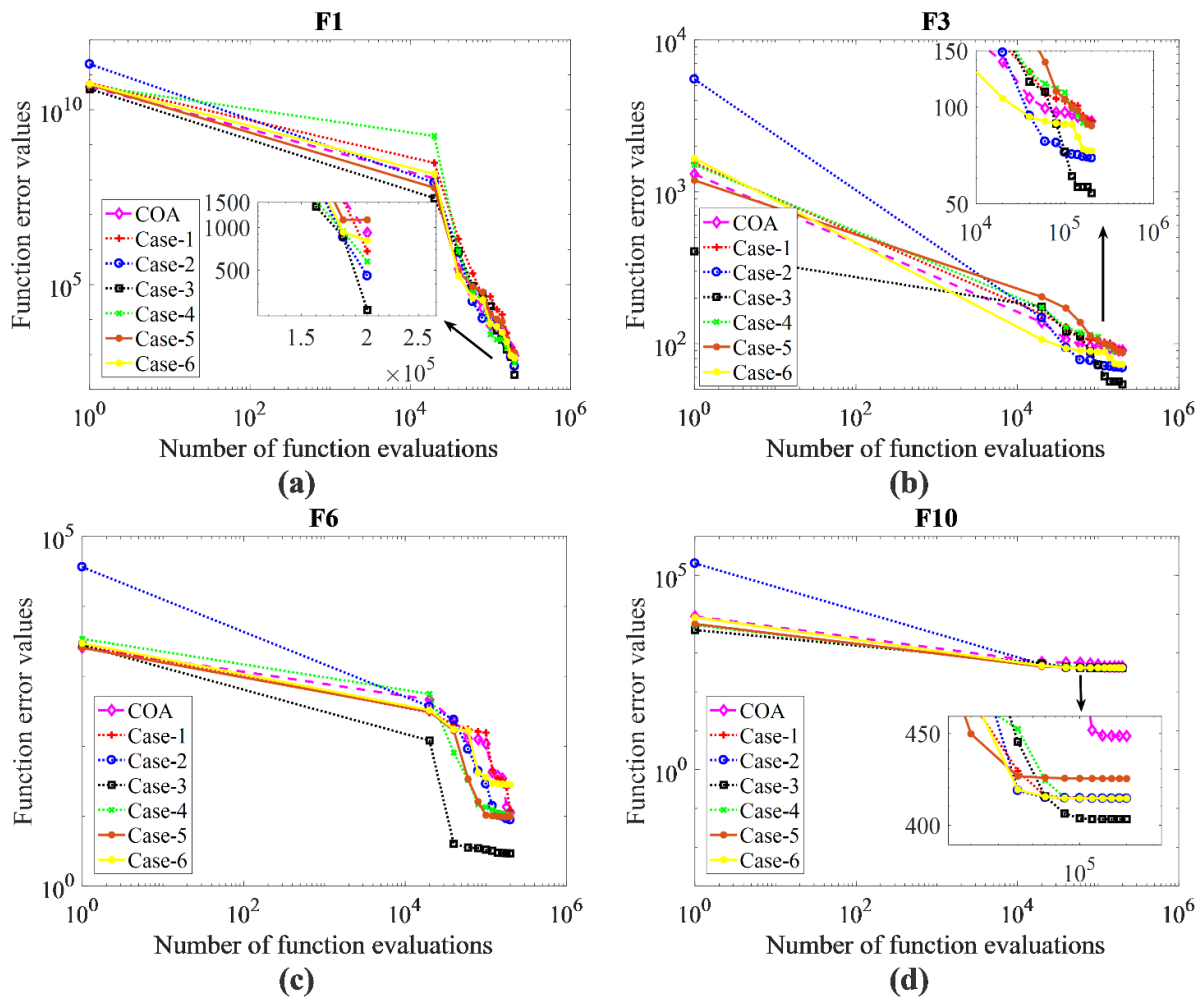


Figure 3. Convergence curves of the COA algorithm and six variations for 20 dimension.

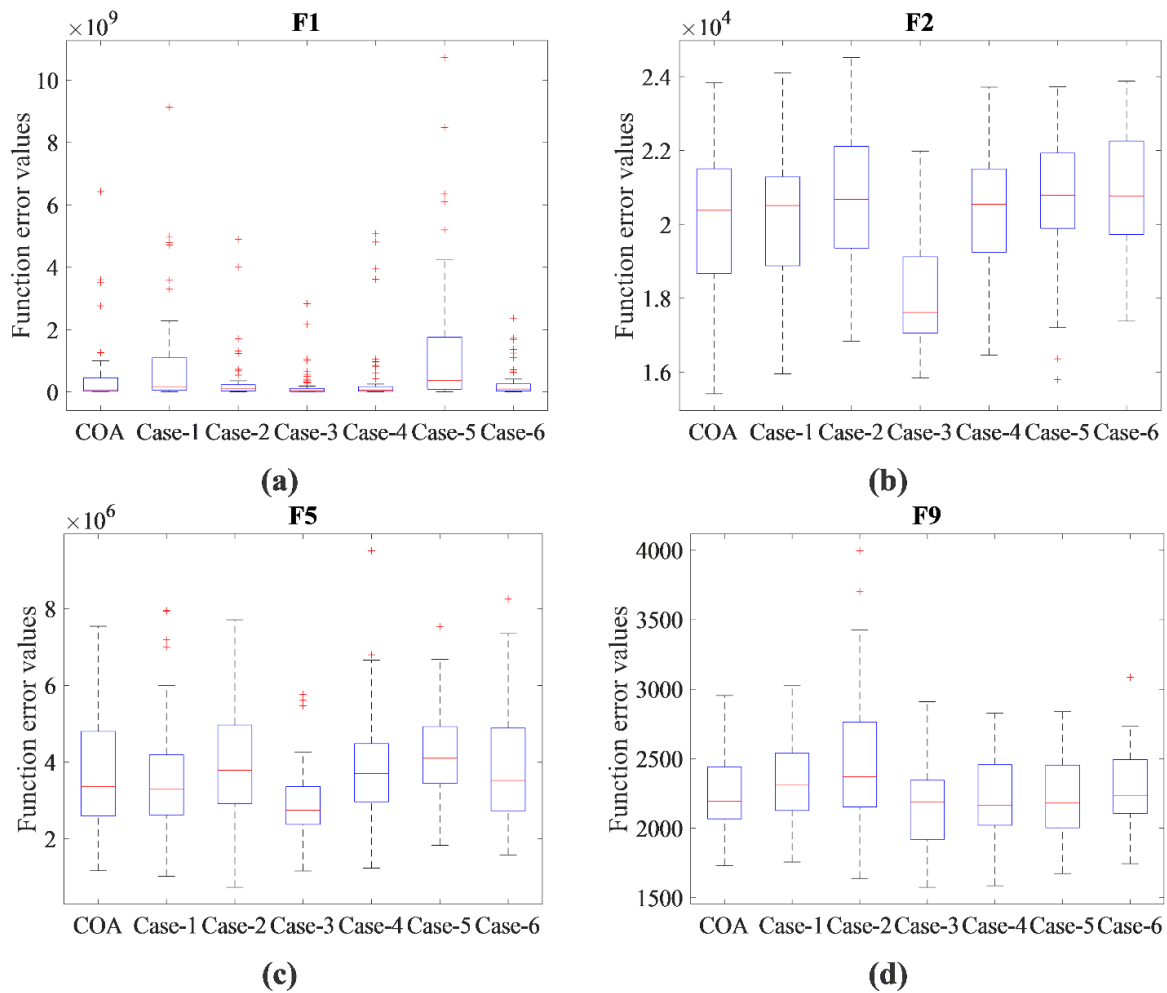


Figure 4. Box-plot graphs of the COA algorithm and six variations for 100 dimension.

Table 3. Parameter range for STP6-120/36, Photowatt-PWP201, and STM6-40/36 PV modules

Parameter	Photowatt-PWP201		STP6-120/36		STM6-40/36	
	<i>lb</i>	<i>ub</i>	<i>lb</i>	<i>ub</i>	<i>lb</i>	<i>ub</i>
<i>a</i>	1	50	1	50	1	60
<i>R_s</i> (Ω)	0	2	0	0.4	0	0.4
<i>R_{sh}</i> (Ω)	0	2000	0	1500	0	1000
<i>I_{pv}</i> (A)	0	2	0	8	0	2
<i>I_{o1}</i> (μA)	0	50	0	50	1	50

3.2. Implementation of the ECOA Algorithm for the PV Parameter Estimation Problem

In this sub-section, the performance of the proposed ECOA is tested in detail for the PV parameter estimation problem. Here, three test cases are considered using three different PV modules including STP6-120/36, Photowatt-PWP201, and STM6-40/36. They have 36 series connected solar cells and operate at 1000 W/m² and the temperatures of 45°, 55°, and 51°, respectively. While the current (*I*) / voltage (*V*) data of the Photowatt-PWP201 can be extracted from (Wu et al., 2018), the *I/V* data of STP6-120/36 and STM6-40/36 can be obtained from (Premkumar et al., 2021). Moreover, the lower and upper bounds of the PV parameters are set to be the same as in the literature and are given in Table 3.

3.2.1. Results of the Photowatt-PWP201 module

The Photowatt-PWP201 module has five unknown

parameters for the single-diode model. To estimate these parameters, the proposed ECOA and the base COA were applied. The optimal parameters obtained from them are listed in Table 4. Accordingly, the ECOA and COA obtained the 0.00238035 and 0.00382927 objective function values, respectively, where the result of the ECOA was 37.8378% lower than the COA. In Table 5, the mean, minimum (min), standard deviation (std), and maximum (max) of the ECOA, COA, and the optimization algorithms reported in the literature are tabulated. From Table 5, the ECOA achieved the best min, mean, and max values among the rivals. Besides, the objective function value of the ECOA was lower by 1.8441%, 15.3275%, 1.8441%, 1.8410%, 1.8451%, and 1.8439% than the ABCTRR (Wu et al., 2018), SMA (Kumar et al., 2020), HDE (Wang et al., 2022), WHHO (Naeijian et al., 2021), RTLBO (Yu et al., 2023), and TLABC (Chen et al., 2018),

respectively. Figure 5 (a) presents the convergence graphs of the proposed ECOA and COA. Accordingly, the ECOA converged faster than the COA. Figure 6 (a) presents the box-plot graphs for the ECOA and COA algorithms, where it was clearly seen that the ECOA

algorithm had a more stable performance than COA. In Figure 7, the I-V and P-V curves of the experimental and calculated data by ECOA are given. These curves clearly show that the proposed algorithm obtained the module parameters with high accuracy.

Table 4. Optimal parameters obtained from ECOA and COA for Photowatt-PWP201 module

Method	a	$R_s (\Omega)$	$R_{sh} (\Omega)$	$I_{pv} (A)$	$I_{o1} (\mu A)$	RMSE
ECOA	48.55280659	1.21074419	996.27014927	1.03047082	3.39999999	0.00238035
COA	50.13811413	1.14691709	777.56118051	1.03591932	5.06086952	0.00382927

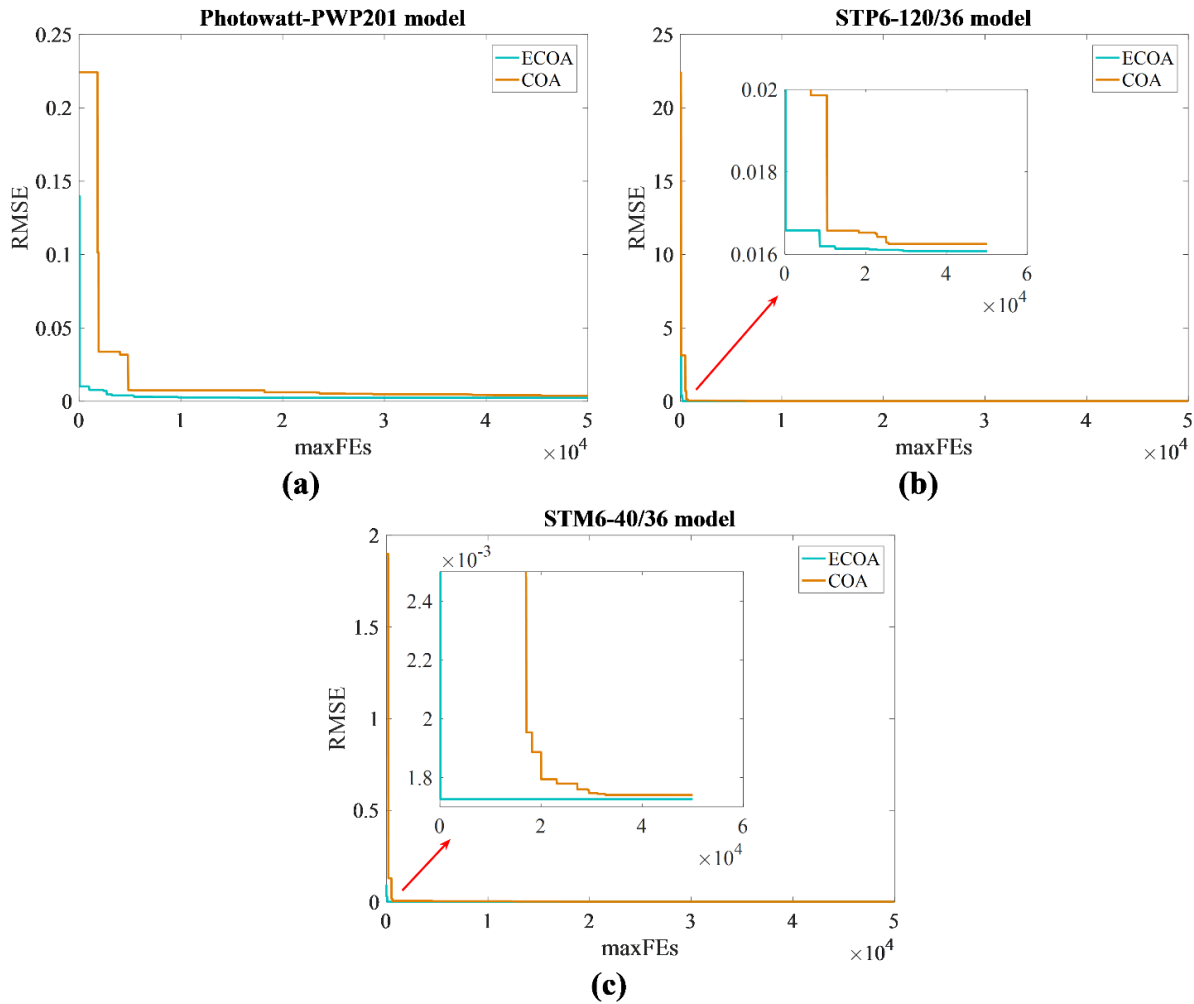


Figure 5. Convergence graphs of the ECOA and COA for (a) Photowatt-PWP201, (b) STP6-120/36, (c) STM6-40/36.

Table 5. Comparison of the results of ECOA with the results of the literature studies for Photowatt-PWP201 module

Method	Min	Mean	Max	Std
ECOA	0.00238035	0.00238637	0.00239472	4.13E-06
COA	0.00382927	0.00842824	0.01223100	1.79E-03
ABCTRR	0.00242508	0.00242508	0.00242508	9.68E-17
SMA	0.00281125	0.00335278	0.10799200	1.08E-02
HDE	0.00242507	0.00242507	0.00242507	3.15E-17
WHHO	0.00242500	0.00242500	0.00242500	N/A
RTLBO	0.00242510	0.00242510	0.00242510	1.80E-17
TLABC	0.00242507	0.00242647	0.00244584	4.00E-06

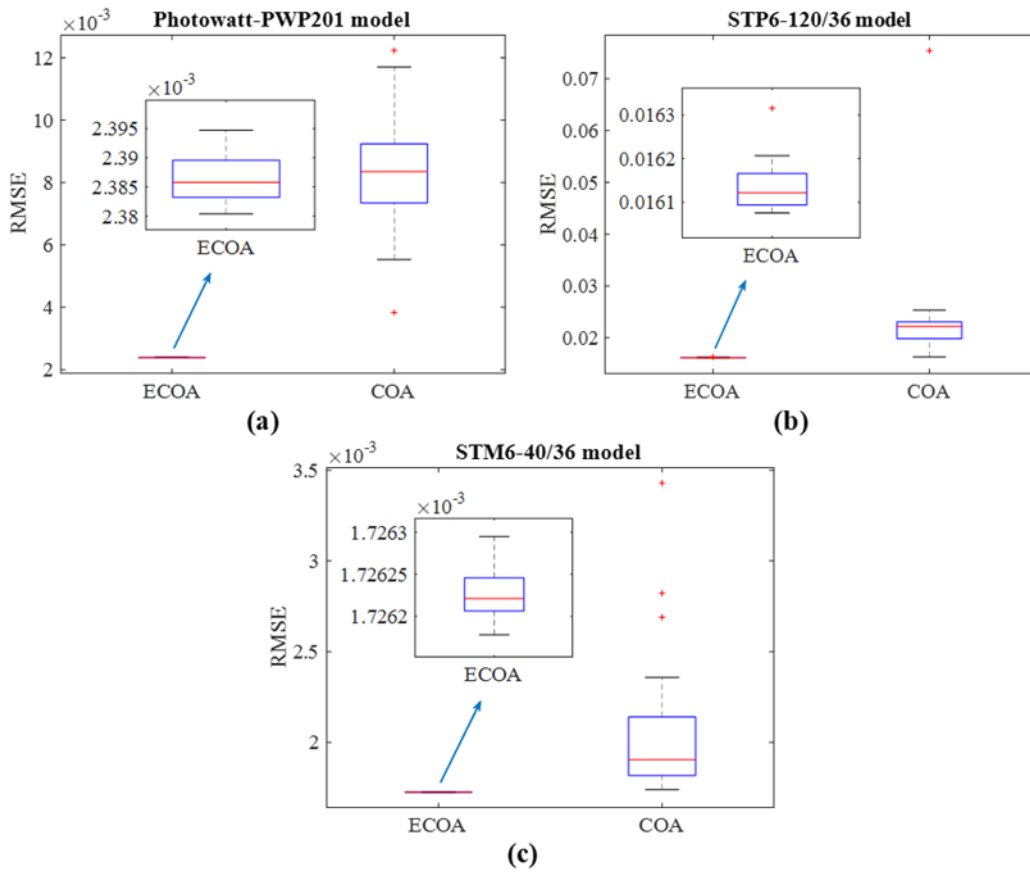


Figure 6. Box-plot graphs of the ECOA and COA for (a) Photowatt-PWP201, (b) STP6-120/36, (c) STM6-40/36.

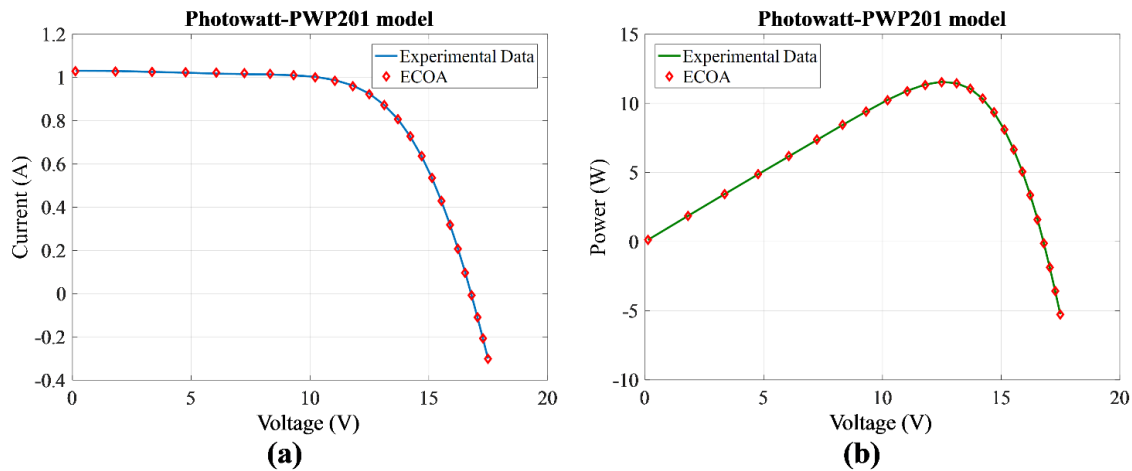


Figure 7. (a) I-V, (b) P-V curves of the experimental and calculated data by ECOA for Photowatt-PWP201.

3.2.2. Results of the STP6-120/36 Module

In order to estimate the parameters of the STP6-120/36 module, the proposed ECOA and base COA were implemented. The optimal parameters obtained from both ECOA and COA are presented in Table 6. From Table 6, the ECOA and COA achieved the 0.01607573 and 0.01625257 objective function values, respectively. In Table 7, the mean, min, std, and max of the ECOA, COA, and the optimization algorithms reported in the literature are listed. From Table 7, the minimum objective value obtained by the ECOA was lower by 1.0880%, 3.1618%, 3.1641%, 3.1618%, and 3.1618%

than the HDE (Wang et al., 2022), RTLBO (Yu et al., 2023), IMFOL (Qaraad et al., 2023), DPDE (Wang et al., 2022), and RLDE (Wang et al., 2022), respectively. Figure 5 (b) shows the convergence curves of the ECOA and COA algorithms. It is seen that the convergence performance of the proposed algorithm was better than its rival. According to Figure 6 (b), the ECOA obtained the lowest minimum, mean, and median objective function values than the COA algorithm. Figure 8 presents the I-V and P-V curves of the experimental and calculated data by ECOA. It shows that the proposed algorithm found the parameters of the STP6-120/36 module most accurately.

Table 6. Optimal parameters obtained from ECOA and COA for STP6-120/36 module

Method	a	$R_s (\Omega)$	$R_{sh} (\Omega)$	$I_{pv} (A)$	$I_{o1} (\mu A)$	RMSE
ECOA	44.19052491	0.18426534	1401.42330369	7.46334747	1.50240004	0.01607573
COA	44.67749123	0.17788827	1020.92793143	7.46882458	1.80016445	0.01625257

Table 7. Comparison of the results of ECOA with the results of the literature studies for STP6-120/36 module

Method	Min	Mean	Max	Std
ECOA	0.01607573	0.01613596	0.01631576	5.34E-05
COA	0.01625257	0.02315716	0.07545616	1.01E-02
HDE	0.01660060	0.01660060	0.01660060	1.86E-16
RTLBO	0.01660100	0.01660100	0.01660100	1.10E-11
DPDE	0.01660060	0.01660060	0.01660060	7.67E-17
RLDE	0.01660060	0.01660060	0.01660060	1.98E-16

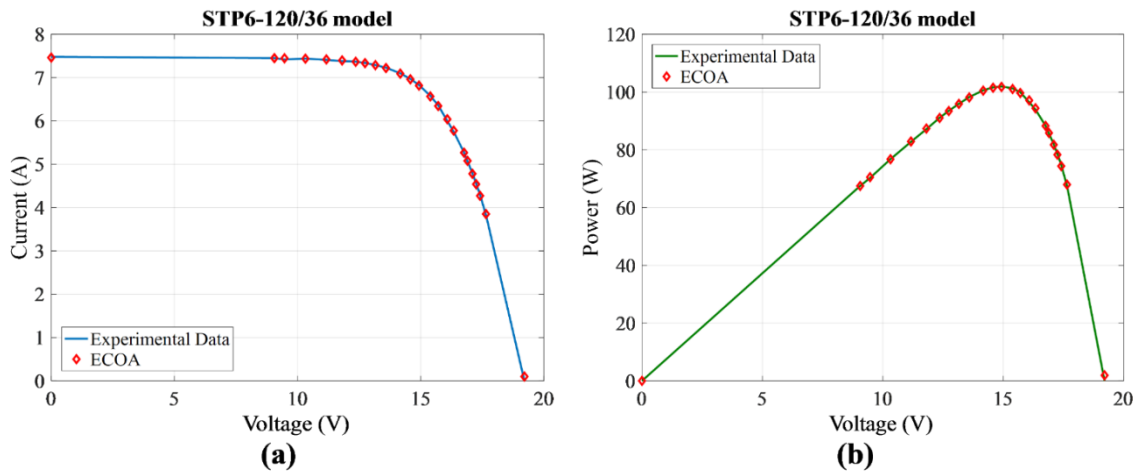


Figure 8. (a) I-V, (b) P-V curves of the experimental and calculated data by ECOA for STP6-120/36.

Table 8. Optimal parameters obtained from ECOA and COA for STM6-40/36 module

Method	a	$R_s (\Omega)$	$R_{sh} (\Omega)$	$I_{pv} (A)$	$I_{o1} (\mu A)$	RMSE
ECOA	56.53886354	0.00000010	603.02089356	1.66323522	2.91000000	0.00172618
COA	55.71193861	0.06329994	578.11228241	1.66374528	2.31970890	0.00174028

Table 9. Comparison of the results of ECOA with the results of the literature studies for STM6-40/36 module

Method	Min	Mean	Max	Std
ECOA	0.00172618	0.00172623	0.00172629	2.85E-08
COA	0.00174028	0.00204472	0.00342965	3.71E-04
HDE	0.00172981	0.00172981	0.00172981	7.89E-18
RTLBO	0.00172980	0.00172980	0.00172980	3.40E-15
IMFOL	0.00188700	0.00303350	0.00467490	8.55E-04
DPDE	0.00172981	0.00172981	0.00172981	1.10E-17
RLDE	0.00172981	0.00172981	0.00172981	1.58E-17

3.2.3. Results of the STM6-40/36 Module

The STM6-40/36 module has five unknown parameters, and the proposed ECOA and base COA were implemented to determine them. The optimal parameters obtained from both ECOA and COA are presented in Table 8. According to Table 8, the ECOA and COA obtained the 0.00172618 and 0.00174028 objective function values, respectively. In Table 9, the mean, min, std, and max of the ECOA, COA, and the optimization algorithms reported in the literature are given. When evaluating the values

given in Table 9, the minimum objective value achieved by the ECOA, was lower by 0.8106%, 0.2102%, 0.2094%, 8.5226%, 0.2102%, and 0.2102% than the COA, HDE (Wang et al., 2022), RTLBO (Yu et al., 2023), IMFOL (Qaraad et al., 2023), DPDE (Wang et al., 2022), and RLDE (Wang et al., 2022), respectively. Figure 5 (c) presents the convergence curves of the ECOA and COA algorithms, where the convergence performance of the ECOA was better than the COA. According to Figure 6 (c), the ECOA showed superior performance than the COA

algorithm, where it achieved the lowest minimum, and mean, and median objective function values than the COA. The I-V and P-V curves of the experimental and calculated data by ECOA are presented in Figure 9. It is seen that the ECOA estimated the unknown parameters of the STM6-40/36 module most accurately.

3.2.4 Sensitivity Analysis

In this study, the aim of the PV parameter estimation problem is to identify the five unknown parameters (a , R_s , R_{sh} , I_{pv} , and I_{o1}) of the STP6-120/36, Photowatt-PWP201, and STM6-40/36 modules. In this section, the sensitivity analysis is performed to identify the most important parameters influencing the PV module's performance. Therefore, the sensitivity analysis was carried out to identify the effect of five unknown parameters (a , R_s , R_{sh} , I_{pv} , and I_{o1}) on the objective function. Within the range of -10%, -5%, +5%, and +10%

of the base case values, the objective function values obtained by varying the determined parameters were recorded. The results of sensitivity analysis using the ECOA algorithm for the Photowatt-PWP201, STP6-120/36, and STM6-40/36 modules are presented in Table 10. Here, the objective function values were calculated in line with the change rates of all parameters given one by one. According to Table 10, it is seen that the change in the a parameter seriously affects the objective function value. While the second parameter that most seriously affects the objective function value is I_{pv} , the third parameter is the I_{o1} affecting the objective function significantly. On the other hand, the parameter that has the least impact on the objective function value is R_{sh} . Thus, the parameters affecting the performance of PV modules were determined.

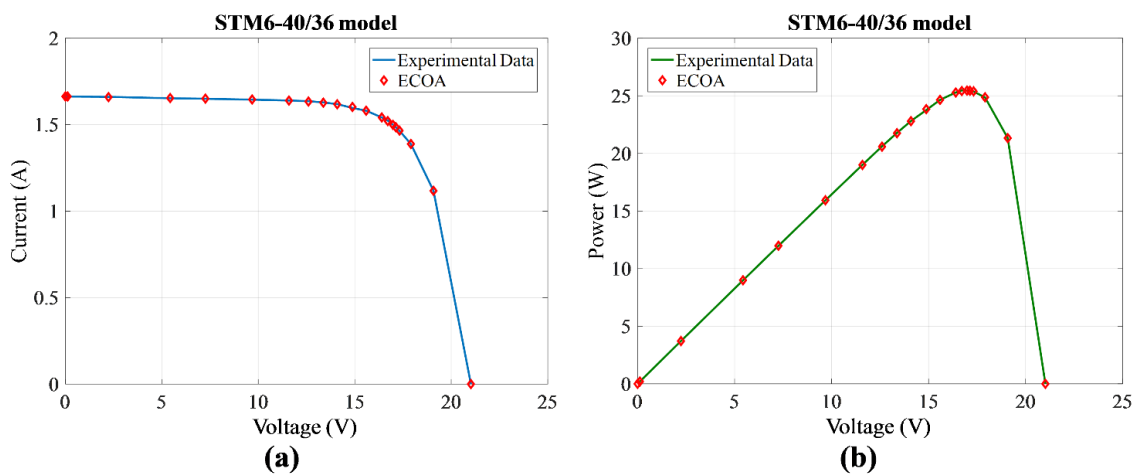


Figure 9. (a) I-V, (b) P-V curves of the experimental and calculated data by ECOA for STM6-40/36.

Table 10. The results of sensitivity analysis using ECOA algorithm for Photowatt-PWP201, STP6-120/36, and STM6-40/36 modules

Type		a	R_s (Ω)	R_{sh} (Ω)	I_{pv} (A)	I_{o1} (μ A)
Photowatt t- PWP201	-10%	1.76417217	0.01424594	0.00283344	0.10312068	0.05788966
	Base	0.00238035	0.00238035	0.00238035	0.00238035	0.00238035
	+10%	1.76417217	0.01424594	0.00283344	0.10312068	0.05788966
STP6- 120/36	-10%	6.19388096	0.10764357	0.01608878	0.74638378	0.15803240
	Base	0.01607573	0.01607573	0.01607573	0.01607573	0.01607573
	+10%	6.19388096	0.10764357	0.01608878	0.74638378	0.15803240
STM6- 40/36	-10%	0.39742699	0.00172618	0.00301994	0.16633338	0.01497132
	Base	0.00172618	0.00172618	0.00172618	0.00172618	0.00172618
	+10%	0.39742699	0.00172618	0.00301994	0.16633338	0.01497132

4. Conclusion

In this paper an enhanced version of the crayfish optimization algorithm including OBL strategies was proposed to determine the parameters of the three PV modules. In this study, three OBL strategies were considered and were applied in different phases of the COA. Accordingly, six COA variations were created, and their performances were compared on solving the CEC2020 benchmark problems in five dimensional search space against the base COA. To evaluate their

results, the statistical analysis methods and the convergence analysis were performed. According to all results obtained from the Friedman and Wilcoxon tests, and the convergence analyzes, the best COA variation was determined and it was called ECOA. On the other hand, to prove the proposed ECOA algorithm on solving the PV parameter estimation problem, the parameters of three PV modules including STP6-120/36, Photowatt-PWP201, and STM6-40/36 were determined using the ECOA and base COA. According to the simulation results,

the proposed ECOA achieved the 37.8378%, 1.0880%, and 0.8106% lower fitness value than the base COA for Photowatt-PWP201, STP6-120/36, and STM6-40/36, respectively. Besides, the results of the ECOA were compared with the results reported in the literature. It shows that the proposed ECOA algorithm achieved more accurate results in estimating model parameters for three PV modules than the results presented in the literature. On the other hand, the sensitivity analysis was conducted to show the effect of the PV model parameters on the objective function. According to the results of the sensitivity analysis, while I_{pv} and a parameters were the most effective parameters on the objective function, the change of R_{sh} has very little effect on the objective function. To sum up, the proposed ECOA is a viable solution to the PV parameter estimation problem since it extracts more accurate and stable parameters with greater efficiency. In future studies, it is considered to apply the ECOA for the estimation of double-diode and triple-diode PV module parameters.

Author Contributions

The percentage of the author contributions is presented below. The author reviewed and approved the final version of the manuscript.

	B.Ö.
C	100
D	100
S	100
DCP	100
DAI	100
L	100
W	100
CR	100
SR	100
PM	100
FA	100

C=Concept, D= design, S= supervision, DCP= data collection and/or processing, DAI= data analysis and/or interpretation, L= literature search, W= writing, CR= critical review, SR= submission and revision, PM= project management, FA= funding acquisition.

Conflict of Interest

The author declared that there is no conflict of interest.

Ethical Consideration

Ethics committee approval was not required for this study because of there was no study on animals or humans.

References

Ali F, Sarwar, A, Bakhsh, FI, Ahmad, S, Shah, AA, Ahmed, H. 2023. Parameter extraction of photovoltaic models using atomic orbital search algorithm on a decent basis for novel accurate RMSE calculation. *Energy Convers Manag*, 277: 116613.
 Ayang A, Wamkeue R, Ouhrouche M, Djongyang N, Salomé NE,

Pombe JK, Ekemb G. 2019. Maximum likelihood parameters estimation of single-diode model of photovoltaic generator. *Renew Energy*, 130: 111-121.
 Ayyarao TS, Kishore GI. 2024. Parameter estimation of solar PV models with artificial humming bird optimization algorithm using various objective functions. *Soft Comput*, 28(4): 3371-3392.
 Cárdenas AA, Carrasco M, Mancilla-David F, Street A, Cardenas R. 2016. Experimental parameter extraction in the single-diode photovoltaic model via a reduced-space search. *IEEE Trans Ind Electron*, 64(2): 1468-1476.
 Çetinbaş İ, Tamyurek B, Demirtaş M. 2023. Parameter extraction of photovoltaic cells and modules by hybrid white shark optimizer and artificial rabbits optimization. *Energy Convers Manag*, 296: 117621.
 Çetinbaş İ. 2024. Parameter Extraction of Single, Double, and Triple-Diode Photovoltaic Models Using the Weighted Leader Search Algorithm. *Glob Chall*, 8(5): 2300355.
 Chen X, Xu B, Mei C, Ding Y, Li K. 2018. Teaching-learning-based artificial bee colony for solar photovoltaic parameter estimation. *Appl Energy*, 212: 1578-1588.
 Chenche LEP, Mendoza OSH, Bandarra Filho EP. 2018. Comparison of four methods for parameter estimation of mono-and multi-junction photovoltaic devices using experimental data. *Renew Sustain Energy Rev*, 81: 2823-2838.
 Duman S, Kahraman H.T, Sonmez Y, Guvenc U, Kati M, Aras S. 2022. A powerful meta-heuristic search algorithm for solving global optimization and real-world solar photovoltaic parameter estimation problems. *Eng Appl Artif Intell*, 111: 104763.
 El-Dabah MA, El-Sehiemy RA, Hasanien HM, Saad B. 2023. Photovoltaic model parameters identification using Northern Goshawk Optimization algorithm. *Energy*, 262: 125522.
 El-Sehiemy R, Shaheen A, El-Fergany A, Ginidi A. 2023. Electrical parameters extraction of PV modules using artificial hummingbird optimizer. *Sci Rep*, 13(1): 9240.
 Ergezer M, Simon D, Du D. 2009. Oppositional biogeography-based optimization. In: *IEEE International Conference on Systems, Man and Cybernetics*, October 11-14, San Antonio, TX, US, pp: 1009-1014.
 Garip Z. 2023. Parameters estimation of three-diode photovoltaic model using fractional-order Harris Hawks optimization algorithm. *Optik*, 272: 170391.
 Isen E, Duman S. 2024. Improved stochastic fractal search algorithm involving design operators for solving parameter extraction problems in real-world engineering optimization problems. *Appl Energy*, 365: 123297.
 Izci D, Ekinci S, Hussien AG. 2024. Efficient parameter extraction of photovoltaic models with a novel enhanced prairie dog optimization algorithm. *Sci Rep*, 14(1): 7945.
 Jia H, Rao H, Wen C, Mirjalili S. 2023. Crayfish optimization algorithm. *Artif Intell Rev*, 56(2): 1919-1979.
 Kumar C, Raj TD, Premkumar M, Raj TD. 2020. A new stochastic slime mould optimization algorithm for the estimation of solar photovoltaic cell parameters. *Optik*, 223: 165277.
 Long W, Jiao J, Liang X, Xu M, Tang M, Cai S. 2022. Parameters estimation of photovoltaic models using a novel hybrid seagull optimization algorithm. *Energy*, 249: 123760.
 Long W, Wu T, Jiao J, Tang M, Xu M. 2020. Refraction-learning-based whale optimization algorithm for high-dimensional problems and parameter estimation of PV model. *Eng Appl Artif Intell*, 89: 103457.
 Maden D, Çelik E, Houssein EH, Sharma G. 2023. Squirrel search algorithm applied to effective estimation of solar PV model

- parameters: a real-world practice. *Neural Comput Appl*, 35(18): 13529-13546.
- Mahdavi S, Rahnamayan S, Deb K. 2018. Opposition based learning: A literature review. *Swarm Evol Comput*, 39: 1-23.
- Naeijian M, Rahimnejad A, Ebrahimi SM, Pourmousa N, Gadsden SA. 2021. Parameter estimation of PV solar cells and modules using Whippy Harris Hawks Optimization Algorithm. *Energy Rep*, 7: 4047-4063.
- Navarro MA, Oliva D, Ramos-Michel A, Haro EH. 2023. An analysis on the performance of metaheuristic algorithms for the estimation of parameters in solar cell models. *Energy Convers Manag*, 276: 116523.
- Ortiz-Conde A, Sánchez FJG, Muci J. 2006. New method to extract the model parameters of solar cells from the explicit analytic solutions of their illuminated I-V characteristics. *Sol Energy Mater Sol Cells*, 90(3): 352-361.
- Premkumar M, Jangir P, Sowmya R, Elavarasan RM, Kumar BS. 2021. Enhanced chaotic JAYA algorithm for parameter estimation of photovoltaic cell/modules. *ISA Trans*, 116: 139-166.
- Qais MH, Hasanien HM, Alghuwainem S. 2020. Transient search optimization for electrical parameters estimation of photovoltaic module based on datasheet values. *Energy Convers Manag*, 214: 112904.
- Qaraad M, Amjad S, Hussein NK, Badawy M, Mirjalili S, Elhosseini MA. 2023. Photovoltaic parameter estimation using improved moth flame algorithms with local escape operators. *Comput Electr Eng*, 106: 108603.
- Rahnamayan S, Tizhoosh HR, Salama MM. 2007. Quasi-oppositional differential evolution. In: *IEEE Congress on Evolutionary Computation*, September 25-28, Singapore, pp: 2229-2236.
- Shaheen AM, Ginidi AR, El-Sehiemy RA, El-Fergany A, Elsayed AM. 2023. Optimal parameters extraction of photovoltaic triple diode model using an enhanced artificial gorilla troops optimizer. *Energy*, 283: 129034.
- Sharma A, Sharma A, Averbukh M, Rajput S, Jatly V, Choudhury S, Azzopardi B. 2022. Improved moth flame optimization algorithm based on opposition-based learning and Lévy flight distribution for parameter estimation of solar module. *Energy Rep*, 8: 6576-6592.
- Tizhoosh HR. 2005. Opposition-based learning: a new scheme for machine intelligence. In: *International Conference on Computational Intelligence for Modelling, Control and Automation and International Conference on Intelligent Agents, Web Technologies and Internet Commerce*, November 28-30, Vienna, Austria, pp: 695-701.
- Wang D, Sun X, Kang H, Shen Y, Chen Q. 2022. Heterogeneous differential evolution algorithm for parameter estimation of solar photovoltaic models. *Energy Rep*, 8: 4724-4746.
- Wang J, Yang B, Li D, Zeng C, Chen Y, Guo Z, Yu T. 2021. Photovoltaic cell parameter estimation based on improved equilibrium optimizer algorithm. *Energy Convers Manag*, 236: 114051.
- Wu L, Chen Z, Long C, Cheng S, Lin P, Chen Y, Chen H. 2018. Parameter extraction of photovoltaic models from measured IV characteristics curves using a hybrid trust-region reflective algorithm. *Appl Energy*, 232: 36-53.
- Xiong G, Gu Z, Mohamed AW, Bouchekara HR, Suganthan PN. 2024. Accurate parameters extraction of photovoltaic models with multi-strategy gaining-sharing knowledge-based algorithm. *Inf Sci*, 670, 120627.
- Yang B, Wang J, Zhang X, Yu T, Yao W, Shu H, Sun L. 2020. Comprehensive overview of meta-heuristic algorithm applications on PV cell parameter identification. *Energy Convers Manag*, 208:112595.
- Yang C, Su C, Hu H, Habibi M, Safarpour H, Khadimallah MA. 2023. Performance optimization of photovoltaic and solar cells via a hybrid and efficient chimp algorithm. *Sol Energy*, 253: 343-359.
- Yu S, Heidari AA, Liang G, Chen C, Chen H, Shao Q. 2022. Solar photovoltaic model parameter estimation based on orthogonally-adapted gradient-based optimization. *Optik*, 252: 168513.
- Yu X, Hu Z, Wang X, Luo W. 2023. Ranking teaching-learning-based optimization algorithm to estimate the parameters of solar models. *Eng Appl Artif Intell*, 123: 106225.
- Yue CT, Price KV, Suganthan PN, Liang JJ, Ali MZ, Qu BY, Biswas PP. 2019. Problem definitions and evaluation criteria for the CEC 2020 special session and competition on single objective bound constrained numerical optimization. *Comput. Intell. Lab., Zhengzhou Univ., Technical Report*, 201911, Henan, China, pp: 65.